K-Ras4A splice variant is widely expressed in cancer and uses a hybrid membrane-targeting motif

Frederick D. Tsai[a], Mathew S. Lopes[a], Mo Zhou[a], Helen Court[a], Odis Ponce[a], James J. Fiordalisi[b,c], Jessica J. Gierut[d], Adrienne D. Cox[b,c], Kevin M. Haigis[d], and Mark R. Philips[a,1]

[a]New York University Perlmutter Cancer Institute, New York University School of Medicine, New York, NY 10016; Departments of [b]Pharmacology and [c]Radiation Oncology, University of North Carolina, Chapel Hill, NC 27599; and [d]Department of Medicine, Harvard Medical School, Boston, MA 02215

The two products of the *KRAS* locus, K-Ras4A and K-Ras4B, are encoded by alternative fourth exons and therefore, possess distinct membrane-targeting sequences. The common activating mutations occur in exons 1 or 2 and therefore, render both splice variants oncogenic. K-Ras4A has been understudied, because it has been considered a minor splice variant. By priming off of the splice junction, we developed a quantitative RT-PCR assay for K-Ras4A and K-Ras4B message capable of measuring absolute amounts of the two transcripts. We found that K-Ras4A was widely expressed in 30 of 30 human cancer cell lines and amounts equal to K-Ras4B in 17 human colorectal tumors. Using splice variant-specific antibodies, we detected K-Ras4A protein in several tumor cell lines at a level equal to or greater than that of K-Ras4B. In addition to the CAAX motif, the C terminus of K-Ras4A contains a site of palmitoylation as well as a bipartite polybasic region. Although both were required for maximal efficiency, each of these could independently deliver K-Ras4A to the plasma membrane. Thus, among four Ras proteins, K-Ras4A is unique in possessing a dual membrane-targeting motif. We also found that, unlike K-Ras4B, K-Ras4A does not bind to the cytosolic chaperone δ-subunit of cGMP phosphodiesterase type 6 (PDE6δ). We conclude that efforts to develop anti–K-Ras drugs that interfere with membrane trafficking will have to take into account the distinct modes of targeting of the two K-Ras splice variants.

Ras | K-Ras | palmitoylation | alternate splicing | oncogene

Ras genes are the most frequently mutated oncogenes in human cancer (1) and therefore, considered among the most important targets for anticancer therapy. The Ras genes encode small GTPases that control cellular pathways that signal for growth, proliferation, and differentiation. Mammalian genomes harbor three Ras genes (*HRAS*, *NRAS*, and *KRAS*) that give rise to four proteins. The 21-kDa gene products of Ras loci share nearly identical sequence homology through the first 165 of 188 to 189 aa. The G domain formed by these 165 aa is the catalytic and switching portion of the protein that binds GDP/GTP and associates with effectors, exchange factors, and GTPase-activating proteins (GAPs) (2). Where the Ras isoforms diverge is in their 24 C-terminal aa, which contain the targeting information for the membrane localization that is necessary for Ras function (3). This hypervariable region (HVR) includes a C-terminal CAAX sequence, which is modified posttranslationally in three steps: farnesylation, AAX proteolysis, and carboxyl methylation of the resulting C-terminal prenylcysteine (4).

Whereas CAAX processing is required for membrane association, it is insufficient for targeting Ras proteins to the plasma membrane (PM) (5). A second signal upstream of the CAAX motif directs Ras proteins to the PM (6). In N-Ras and H-Ras, the second signal consists of one or two cysteine residues that serve as sites of palmitoylation. K-Ras4B lacks palmitoylation but instead, contains a series of lysines that constitutes a polybasic region (PBR) capable of interacting, without additional modification, with the inner leaflet of the PM through an electrostatic interaction. Unlike CAAX processing, the second signals are reversible, because the palmitoyl thioester modifications of N-Ras and H-Ras are labile and because the charge of the

PBR of K-Ras4B can be diminished by phosphorylation of a serine interposed within the sequence (7).

The *KRAS* gene is unique among Ras genes in that it encodes two gene products by alternative splicing. The two transcripts differ by use of two alternative fourth exons and therefore, are designated K-Ras4A and K-Ras4B. The alternative fourth exons encode the HVRs of the proteins that are responsible for membrane targeting. Whereas K-Ras4B lacks a site of palmitoylation, K-Ras4A is palmitoylated (8). K-Ras4A mRNA is expressed early in embryogenesis and differentially expressed in adult tissues (9). In humans, K-Ras4A is reported to be expressed in the gastrointestinal tract and to a lesser degree, kidney, lung, and other tissues of endodermal origin as well as some mesodermal derivatives but not at all in nervous system or skeletal muscle (10). Although the *KRAS* gene locus is essential for mouse embryonic development, expression of K-Ras4A is not essential, because targeted KO of exon 4A in mice resulted in no impairment in survival, growth, or fertility (11). Whether K-Ras4A can substitute for K-Ras4B in development has not been tested.

The K-Ras4A splice variant is conserved in eukaryotes (Fig. S1). The evolution of two splice variants of *KRAS* and the differential expression of the two transcripts suggest distinct functions. However, no unambiguous evidence for differential function has been reported. It is clear that activated K-Ras4A is capable of transforming cells. Notably, K-Ras4A was the first splice variant discovered by virtue of it being the transforming gene carried by the Kirsten murine sarcoma virus (12). Mutated K-Ras4A has been shown to activate Raf-1 and signal through the MAPK pathway much more efficiently than oncogenic H-Ras and N-Ras, and the ability of oncogenic K-Ras4A to induce

Significance

The *KRAS* oncogene is mutated more frequently in human cancer than any other. The *KRAS* transcript is alternatively spliced to give rise to two products, K-Ras4A and K-Ras4B, both of which are oncogenic when *KRAS* is mutated. We detected significant amounts of each transcript in human tumor cells and colorectal carcinomas. We found that K-Ras4A is targeted to the plasma membrane by dual targeting motifs distinct from those of K-Ras4B. Because interfering with membrane association of Ras proteins remains one of the most attractive approaches to anti-Ras therapy, efforts in this direction will have to disrupt both the K-Ras4A and the K-Ras4B membrane-targeting pathways.

CELL BIOLOGY

formation of transformed foci and enable anchorage-independent growth is significantly greater than that of oncogenic K-Ras4B expressed at the same level (13). A recent study suggested that the presence of oncogenic K-Ras4A was necessary to initiate tumor formation and growth in a mouse model of induced lung carcinogenesis through *KRAS* mutation (14). Importantly, because the mutations found in human cancer that render *KRAS* constitutively active are located in exons 1 and 2, both splice variants expressed from a mutated allele will encode oncogenic proteins. Because mRNA levels of K-Ras4A have been reported to be lower than those of K-Ras4B (9, 10, 15), the former has been considered the minor splice variant of the *KRAS* locus and largely ignored in the vast literature on K-Ras.

In this study, we develop superior tools to detect expression of K-Ras4A at the message and protein levels, revisit the question of relative expression of the K-Ras splice variants in human cancer, and conclude that a significant amount of K-Ras4A is expressed in colorectal carcinoma. We also show that K-Ras4A is unique among Ras isoforms in that it contains two targeting signals in its HVR, which act redundantly to direct K-Ras4A to the PM, where it is able to signal.

Results

K-Ras4A Is Expressed in Human Cancer. The only difference in K-Ras4A vs. K-Ras4B mRNA is the presence or absence of exon 4A (Fig. 1A). Previous studies of the relative abundance of the two transcripts used primers that initiate in exons 1 (forward) and 4B (reverse), such that an amplification product was obtained with either transcript, and the splice variant assignment was made based on the size of the product (10). We found that, using such primers and plasmid-encoded cDNAs as templates, the amplification efficiency varied dramatically depending on the presence or absence of exon 4A, such that the relative abundance of size-defined amplification products does not accurately reflect the relative abundance of the two transcripts. Accordingly, we developed a reverse primer that initiates across the exon 3/4B splice junction, such that a product is observed only when the template lacks exon 4A (Fig. 1A). A second reverse primer in the 4A exon produced a 4A-specific product. Using cDNA of each K-Ras splice variant cloned into a pEGFP vector backbone, we generated standard curves for each quantitative PCR (qPCR) reaction, such that we were able to determine the absolute concentrations of each template as a function of the amplification products (Fig. S2). cDNAs from a variety of human cancer cell lines derived from different tumors with or without *KRAS* mutations were used to study the relative abundance of K-Ras4A and K-Ras4B transcripts. Although K-Ras4B message was more abundant overall, the K-Ras4A transcript was expressed in every cell line examined (Fig. 1B), with particular prominence in cell lines derived from colon carcinoma and melanoma. K-Ras4A accounted for 10–50% of total *KRAS* transcripts, levels significantly higher than previously reported (10, 15, 16). The relative abundance of the two transcripts did not seem to correlate with K-Ras mutations. To better determine if the *KRAS* mutational status affects splicing, we examined isogenic cell line pairs for the colon cancer cell lines DLD-1 and HCT116 (17). We did not observe any difference in the relative abundance of the two mRNAs among cells that harbor WT vs. mutated *KRAS* alleles (Fig. S3).

To confirm that our observations with established cancer cell lines, which are susceptible to genetic drift in culture, reflected the status of primary human tumors, we examined by RT-qPCR fresh frozen tissue from 17 colorectal adenocarcinomas. Strikingly, the relative abundance of K-Ras4A and K-Ras4B mRNA was more equal than that observed in cell lines. Indeed, over the entire set of samples, the relative abundance of the two transcripts was equal (Fig. 1C).
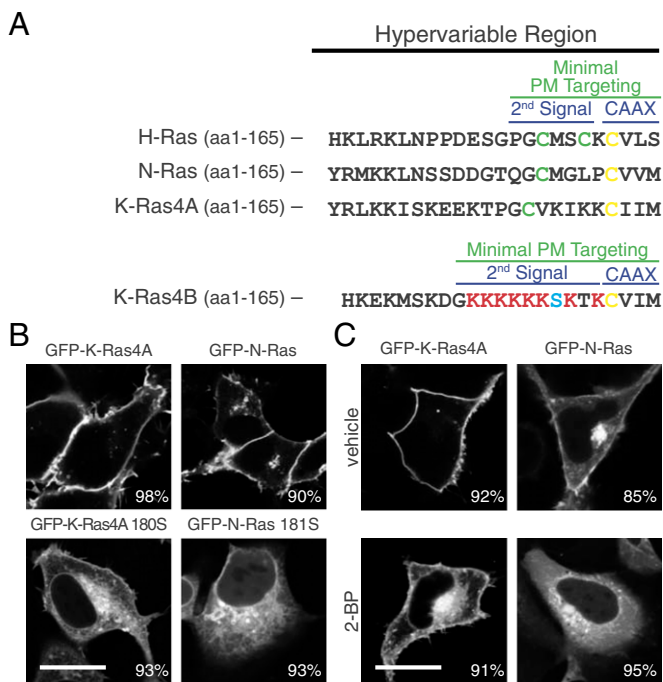
To determine if our RT-qPCR findings translate into protein expression, we developed a rabbit polyclonal antibody specific
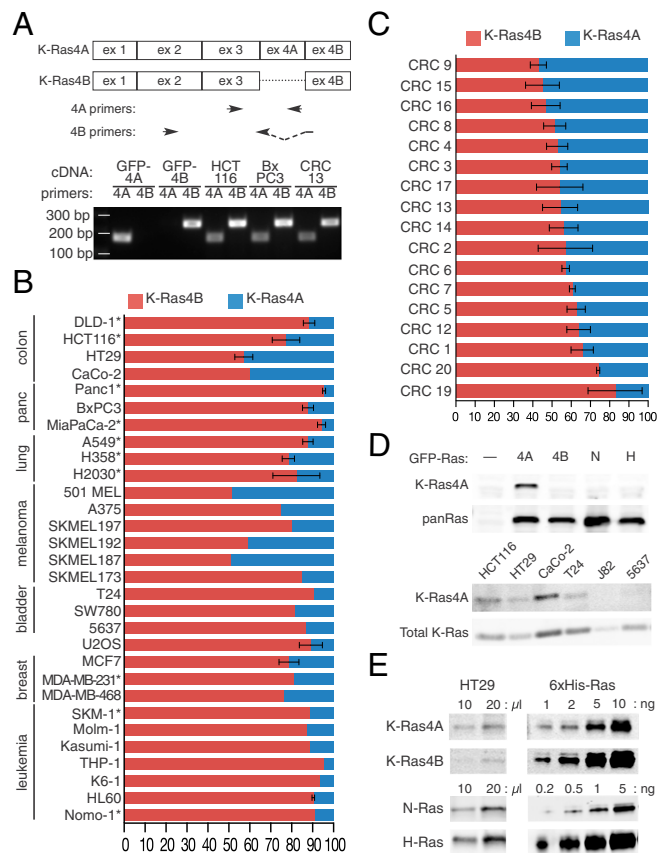
Fig. 1. K-Ras4A is expressed in human cancer. (*A, Upper*) Schematic of K-Ras4A and K-Ras4B mRNA sequences with locations of primer pairs used for RT-PCR indicated. Reverse primers were designed to prime in exon 4A or the exon 3/4B splice. (*A, Lower*) Representative agarose gel showing RT-PCR products using 4A- or 4B-specific primer pairs and the indicated cDNA template. (*B* and *C*) Quantification of K-Ras isoform transcripts. cDNA from total RNA extracts was generated from (*B*) indicated cancer cell lines or (*C*) fresh frozen colorectal tumors, and qPCR was performed using the primer pairs indicated in *A*. Results are graphed as percentage of K-Ras isoform transcript relative to total K-Ras mRNA. In *B*, asterisks indicate cell lines with mutated *KRAS*. In *B* and *C*, the data shown are the means of two to three independent determinations (error bars representing SD are shown when *n* = 3). (*D, Upper*) Validation of the specificity of an anti–K-Ras4A antibody. (*D, Lower*) Lysates from indicated cancer cell lines (HCT116, HT29, and CaCo-2 from colorectal carcinoma and T24, J82, and 5637 cells from urothelial carcinoma) were immunoprecipitated for Ras and immunoblotted using the K-Ras4A–specific or antitotal K-Ras antibodies. (*E*) Lysates of 10^7 HT29 cells were immunoprecipitated for total Ras, and the indicated amounts of eluate (total volume = 133 μL) were immunoblotted for the indicated Ras isoforms alongside a standard curve generated with bacterially expressed 6xHis-tagged Ras proteins.

for K-Ras4A (Fig. 1D). Using this anti–K-Ras4A antibody, we were able to detect the presence of K-Ras4A protein in cell lines derived from colorectal and bladder tumors (Fig. 1 *D* and *E*). Using isoform-specific anti-Ras antibodies (Fig. S4) and standard curves generated with bacterially expressed 6xHis-Ras proteins (Fig. S5), we determined that the cellular contents of K-Ras4A, K-Ras4B, N-Ras, and H-Ras in HT29 cells were 2.6, 1.2, 2.8, and 0.7 $ng/10^6$ cells, respectively (Fig. 1E). Thus, K-Ras4A is relatively well-expressed in human colorectal cancer cell lines and tissues and perhaps, other human cancers.

K-Ras4A Uses Two Targeting Motifs to Traffic to the PM. Like N-Ras and H-Ras, the HVR of K-Ras4A contains a cysteine that has been shown to be palmitoylated (8). Indeed, the HVR of K-Ras4A shows sequence homology to that of N-Ras (Fig. 2A).

A
Hypervariable Region

Minimal PM Targeting
2nd Signal | CAAX

H-Ras (aa1-165) – HKLRKLNPPDESGPGCMSCKCVLS
N-Ras (aa1-165) – YRMKKLNSSDDGTQGCMGLPCVVM
K-Ras4A (aa1-165) – YRLKKISKEEKTPGCVKIKKCIIM

Minimal PM Targeting
2nd Signal | CAAX

K-Ras4B (aa1-165) – HKEKMSKDGKKKKKKSKTKCVIM

B

GFP-K-Ras4A 98% | GFP-N-Ras 90%
GFP-K-Ras4A 180S 93% | GFP-N-Ras 181S 93%

C

GFP-K-Ras4A 92% | GFP-N-Ras 85% (vehicle)
91% | 95% (2-BP)

Fig. 2. K-Ras4A is targeted to the PM, even in the absence of palmitoylation. (A) Sequences of the C-terminal HVRs of four Ras proteins. The farnesylated cysteine of the CAAX motif is indicated in yellow, whereas the cysteines serving as sites of palmitoylation are in green. For K-Ras4B, the polybasic domain is in red, with blue indicating the site of phosphorylation. (B) HEK293 cells were transfected with the indicated constructs and imaged live by confocal microscopy. (C) HEK293 cells were transfected with GFP-K-Ras4A or GFP-N-Ras and treated with 2-bromopalmitate (2-BP; 50 μM) or vehicle (DMSO) for 3 h before imaging live by confocal microscopy. All images are representative of the indicated percentage of >50 live fluorescent cells examined. (Scale bar: 10 μm.)

N-Ras and H-Ras as well as other palmitoylated small GTPases are expressed on both the PM and Golgi apparatus (18). In striking contrast, when we imaged live cells expressing K-Ras4A fused to GFP, we found that GFP-K-Ras4A localized exclusively to the PM (Fig. 2B). Because cysteine 180 is the only cysteine in the K-Ras4A HVR apart from the farnesylated CAAX cysteine and because Laude and Prior (8) found [3H]palmitate incorporation into GFP extended with the HVR only, one site of K-Ras4A palmitoylation is thought to be cysteine 180. To confirm that palmitoylation of cysteine 180 is required for K-Ras4A membrane association, we mutated the presumed palmitate acceptor site to serine. GFP-K-Ras4A180S localized extensively to internal membranes, indicating that palmitoylation is, indeed, required for efficient targeting of K-Ras4A to the PM (Fig. 2B). However, a portion of GFP-K-Ras4A180S was clearly observed at the PM, which is in stark contrast to GFP-N-Ras181S (Fig. 2B). Treatment of cells expressing GFP-K-Ras4A with 2-bromopalmitate, an inhibitor of palmitoylation, led to increased expression on endomembrane but failed to block expression on the PM. In contrast, GFP-N-Ras was blocked completely from the PM under the same conditions (Fig. 2C). Thus, despite a role for palmitoylation in K-Ras4A membrane trafficking, another targeting signal in K-Ras4A is able to direct it to the PM in the absence of palmitoylation.
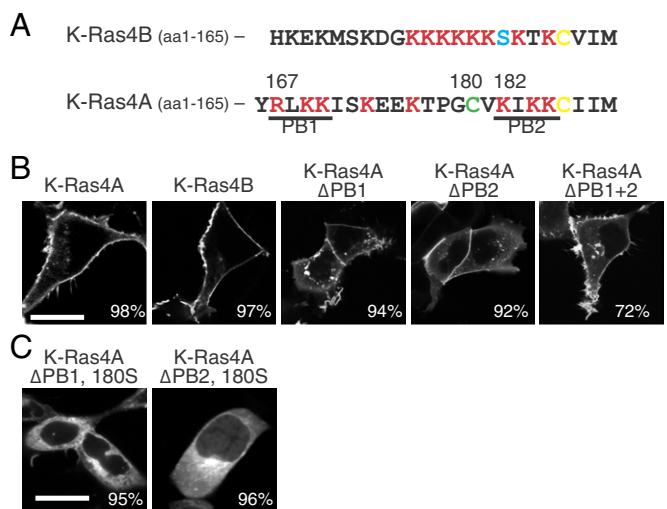
Analysis of the C-terminal sequence of K-Ras4A revealed two clusters of positively charged residues (PB1 and PB2), suggesting that, like K-Ras4B, K-Ras4A may contain PBRs active in membrane targeting (Fig. 3A). The observation that the steady-state localization of GFP-K-Ras4A was identical to that of

K-Ras4B (Fig. 3B) but differed from that of N-Ras (Fig. 2B) and H-Ras (5) is consistent with a functional PBR. Indeed, Laude and Prior (8) previously reported that PB2 stabilizes the interaction of the palmitate on K-Ras4A with the PM. We hypothesized that, when palmitoylation of K-Ras4A was absent, PB1 and/or PB2 are sufficient to direct K-Ras4A to the PM. To test this hypothesis, we mutated the positively charged residues in each PBR to electrostatically neutral glutamines either singly or combined. Removal of either PBR alone (ΔPB1 or ΔPB2) did not significantly affect K-Ras4A localization (Fig. 3B). However, removal of both PBRs (ΔPB1+2) changed the steady-state distribution of K-Ras4A to the PM and Golgi apparatus (Fig. 3B and Fig. S6). Thus, GFP-K-Ras4A(ΔPB1+2) was expressed in a pattern identical to that of GFP-N-Ras and GFP-H-Ras, the Ras isoforms that depend absolutely on palmitoylation for PM expression.

Next, we removed the site of palmitoylation combined with a PBR, so that only one PBR remained. The loss of both PB1 and palmitoylation resembled the C180S mutant alone, albeit with diminished but not absent PM localization (Fig. 3C). In contrast, loss of PB2 and palmitoylation completely removed K-Ras4A from the PM and resulted in localization exclusively to endomembrane and cytosol, confirming that both palmitoylation and PB2 are required for efficient targeting to the PM.

To rule out the possibility that one or both PBRs are required for palmitoylation of K-Ras4A, we performed metabolic labeling with [3H]palmitic acid. We found that K-Ras4A lacking cysteine 180 failed to incorporate any [3H]palmitic acid (Fig. S7), thus showing for the first time, to our knowledge, that cysteine 180 is the only site of palmitoylation in K-Ras4A. Mutation of the PBRs, either singly or together, did not affect the steady-state incorporation of palmitate (Fig. S7). Thus, the PBRs do not affect the efficiency of palmitoylation of K-Ras4A expressed by transfection, suggesting that the PBRs have an alternative direct role in the membrane targeting of the protein.

K-Ras4B but Not K-Ras4A Binds the δ-Subunit of cGMP Phosphodiesterase Type 6. In addition to vesicular transport, the trafficking of Ras proteins between membrane compartments involves the transfer

A
K-Ras4B (aa1-165) – HKEKMSKDGKKKKKKSKTKCVIM

K-Ras4A (aa1-165) – YRLKKISKEEKTPGCVKIKKCIIM
167 ... 180 182
PB1 ... PB2

B

K-Ras4A 98% | K-Ras4B 97% | K-Ras4A ΔPB1 94% | K-Ras4A ΔPB2 92% | K-Ras4A ΔPB1+2 72%

C

K-Ras4A ΔPB1, 180S 95% | K-Ras4A ΔPB2, 180S 96%

Fig. 3. Polybasic domains contribute to K-Ras4A PM localization. (A) Sequences of the K-Ras4B and K-Ras4A C-terminal HVRs with PBRs (PB1 and PB2) underlined. Features are indicated as described in Fig. 2A. (B and C) HEK293 cells were transfected with the indicated constructs and imaged live by confocal microscopy. ΔPB1 and ΔPB2 mutations indicate 167–170 QLQQ and 182–185 QIQQ substitutions, respectively. ΔPB1+2 indicates combined substitutions at both PBRs. All images are representative of the indicated percentage of >50 live fluorescent cells examined. (Scale bar: 10 μm.)

of lipidated, hydrophobic molecules across the aqueous environment of the cytosol and therefore, requires cytosolic chaperones capable of shielding their lipid moieties. One of these is the δ-subunit of cGMP phosphodiesterase type 6 (PDE6δ) (19). We confirmed (Fig. 4) that K-Ras4B and N-Ras but not H-Ras can be extracted from membranes by overexpression of PDE6δ (19, 20). Strikingly, PDE6δ did not function as a cytosolic chaperone for K-Ras4A (Fig. 4). Thus, despite identical steady-state localizations at the PM (Fig. 3B), K-Ras4B and K-Ras4A have distinct mechanisms of subcellular trafficking.

K-Ras4A Localization Signals Affect Its Downstream Signaling. Disruption of neither palmitoylation (180S) nor the PBRs (ΔPB1+2) alone affected the EGF-stimulated GTP loading of K-Ras4A (Fig. 5A), supporting the observation that either form of second signal can deliver K-Ras4A to the PM, where it will encounter the exchange factor SOS. Curiously, when only PB2 was removed (ΔPB2), GTP loading was diminished by 40% (P < 0.02), and when PB2 was removed in conjunction with loss of palmitoylation (ΔPB2+180S), GTP loading was inhibited by 70% (P < 0.005). Thus, PB2 plays a critical role in nucleotide exchange on K-Ras4A with or without palmitoylation.

The C-terminal mutations did not affect the constitutively GTP-loaded state of 12V mutations of K-Ras4A (Fig. S8A). K-Ras4A12V180S was significantly impaired in driving ERK phosphorylation relative to K-Ras4A12V, although phospho-ERK levels were higher than controls, indicating diminished but persistent signaling (Fig. 5B). Mutation of either PBR alone did

not affect phospho-ERK levels, and although mutation of both PBRs consistently decreased phospho-ERK levels, this difference was not significant (n = 4) (Fig. 5B). Mutation of either PBR combined with loss of palmitoylation significantly reduced ERK phosphorylation to the baseline level found in cells transfected with an empty vector. These levels were similar to those of K-Ras4A12V186S that cannot be prenylated (Fig. 5B). These results were corroborated with assays of anchorage-independent growth of rodent fibroblasts (Fig. 5C and Fig. S8 B and C). Colony growth in soft agar was reduced but not eliminated by removal of either PBR alone (ΔPB1 or ΔPB2) or combined (ΔPB1+2) or abolition of palmitoylation (180S). In contrast, removal of PB2 and the palmitoylation site resulted in no more colonies than vector alone. Thus, the ability of K-Ras4A to maximally drive MAPK signaling and transform cells requires both palmitoylation and at least one PBR, and removal of one or the other targeting motifs diminishes but does not abolish activity.

To explore the downstream signaling of K-Ras4A in a more biologically relevant context, we used PC12 cells, which differentiate in response to expression of activated Ras proteins in the absence of growth factor stimulation. Expression of GFP-tagged K-Ras4A12V, N-Ras12D, and H-Ras12V all induced differentiation of PC12 cells as determined by neurite outgrowth, but when palmitoylation was eliminated by mutation, only K-Ras4A12V retained the ability to stimulate neurite outgrowth (Fig. 5D). Thus, K-Ras4A behaves in a manner strikingly different from that of H-Ras and N-Ras with regard to the requirement for palmitoylation. Like elimination of palmitoylation, loss of the PBRs did not affect the ability for K-Ras4A12V to induce PC12 cell differentiation (Fig. 5E). The loss of palmitoylation in conjunction with PB1 (ΔPB1+180S) reduced the ability to stimulate neurite outgrowth by 50%, indicating that PB2 can function in isolation. Strikingly, the combined loss of palmitoylation and PB2 (ΔPB2+180S) resulted in a K-Ras4A protein that was totally inactive in stimulating PC12 differentiation, supporting the conclusion that PB2 is essential for K-Ras4A signaling (Fig. 5E). Interestingly, although the HVR mutations that completely blocked delivery to the PM also blocked signaling, there was no one-to-one correlation between the extent of PM localization and signaling; for example, whereas ΔPB1 and ΔPB2 localized to the PM to similar extents (Fig. 3B), 12V ΔPB1 was two times as efficient as 12V ΔPB2 in activating MAPK (Fig. 5A). Nevertheless, taken together, the signaling data are consistent with the observed localization patterns of K-Ras4A and support the idea that K-Ras4A contains two independently acting membrane-targeting signals, either one of which is sufficient for signal output.

Discussion

Our data reveal expression of K-Ras4A mRNA in all 30 human cell lines examined. Although K-Ras4B message was present at higher levels in the majority of these, in 40% of these lines, the K-Ras4A transcript exceeded 20% of total K-Ras message, and in several, the mRNA levels for the two splice variants were relatively equal. More compelling was the analysis of fresh colorectal tumors, where expression levels of the two transcripts were equal over a panel of 17 samples. It is likely that our results differ from those previously reported (10, 15, 16), because we used splice variant-specific RT-qPCR primers and measured absolute mRNA levels against a standard curve generated with each experiment. Our results analyzing mRNA were supported by studies of protein expression. We developed a K-Ras4A–specific antibody that permitted the first demonstration, to our knowledge, of K-Ras4A protein in cancer cell lines. Using standard curves generated with recombinant protein, we were able to measure the absolute levels of all four Ras proteins in HT29 colorectal cancer cells that harbor a mutant *KRAS* gene and found that K-Ras4A was expressed at the same level as

GFP-Ras + mCherry-PDE6δ   GFP-Ras
GFP   mCherry
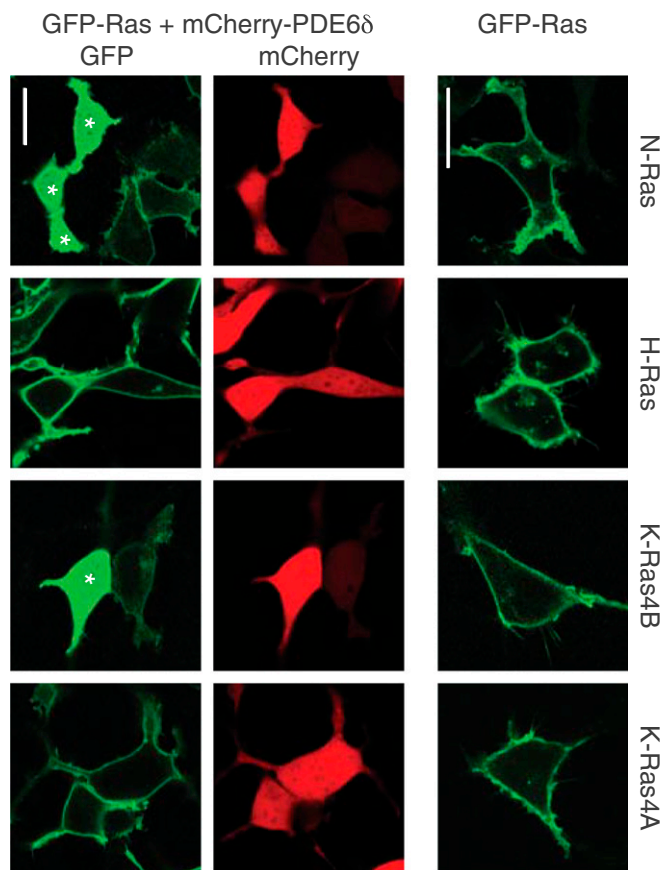
Fig. 4. PDE6δ fails to extract K-Ras4A from membranes. HEK293 cells were transfected with the indicated GFP-tagged Ras proteins (*Right*) alone or (*Left* and *Center*) along with mCherry-PDE6δ and imaged live 24 h later. Asterisks indicate cells in which PDE6δ extracted Ras from membranes. (Scale bar: 10 μm.)
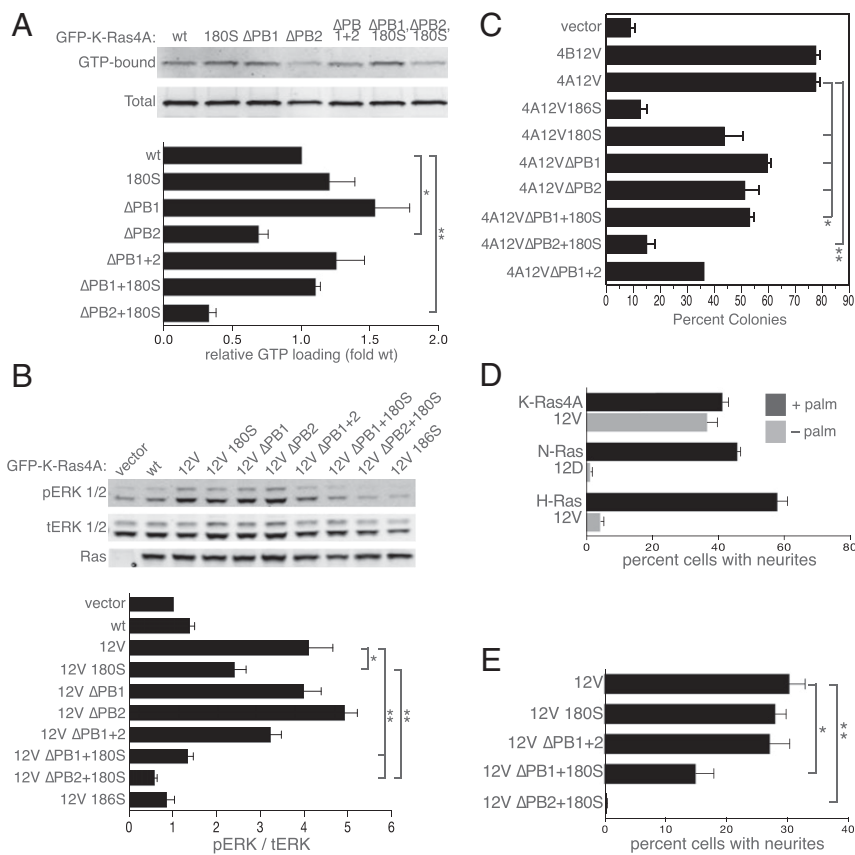
Fig. 5. Dual membrane-targeting signals support K-Ras4A signaling. (*A*) HeLa cells expressing the indicated GFP-K-Ras4A constructs were serum-starved overnight and then stimulated with EGF (10 ng/mL) for 3 min. GTP-bound Ras was affinity-purified from cell lysates with GST–Ras binding domain (RBD). Ras was detected by immunoblot with a pan-Ras antibody from both GST-RBD pull downs and lysates. *Lower* shows quantification of GTP loading, with results presented as fold change in GTP-bound K-Ras4A normalized to expression. Values are mean ± SEM (*n* = 5). (*B*) Lysates of HeLa cells expressing the indicated constitutively active GFP-K-Ras4A12V constructs were immunoblotted for phospho-ERK, total ERK, and Ras. *Lower* shows quantification of phospho-ERK presented as a ratio to total ERK normalized to GFP-Kras4A expression. Values are mean ± SEM (*n* = 4). (*C*) Anchorage-independent growth of NIH 3T3 fibroblasts stably expressing the indicated constructs. Results are shown as the percentages of cells that form colonies and plotted as mean ± SEM (*n* = 4). (*D*) PC12 cells were transfected with the indicated GFP-Ras constructs, with + palm indicating the palmitoylated form and − palm indicating palmitoylation-deficient mutants 180S, 181S, or 181,4SS for K-Ras4A, N-Ras, or H-Ras, respectively. After 3 d, GFP-positive cells were scored for neurites with lengths ≥1.5 times the diameter of the cell soma. Data plotted are percentages of cells with neurites (mean ± SEM; *n* = 3). (*E*) PC12 cells were transfected with the indicated GFP-K-Ras4A constructs and scored for neurite processes as in *C*. *P = 0.01; **P = 0.001 (Student's *t* test).

N-Ras and in excess of K-Ras4B and H-Ras. Our data show that K-Ras4A is expressed in human cancer cells and thereby, dispel the widely held notion that the K-Ras4A splice variant does not contribute to oncogenesis or tumor maintenance when the *KRAS* gene sustains an activating mutation.

The conservation of the *KRAS* 4A exon through evolution and the expression of K-Ras4A in human tissues suggest nonredundant functions for the two splice variants; however, the evidence for distinct activities is limited and often contradictory. Both splice variants of K-Ras are highly transforming in standard assays using rodent fibroblasts, and in one study, K-Ras4A was more active than K-Ras4B (13). Perhaps the most compelling argument for a role for K-Ras4A in oncogenesis is the fact that the transforming gene carried by the Kirsten rat sarcoma virus is the K-Ras4A cDNA (12).

Whereas the *NRAS* and *HRAS* loci are dispensable for mouse development, the *KRAS* locus is essential (21–23). However, mice homozygous for the *HRAS* cDNA knocked into the *KRAS* locus are viable (24), suggesting that the essentiality of the *KRAS* locus is, at least in part, because of gene expression patterns rather than differential function of the gene products. Exon 4A is also dispensable with regard to mouse development (11), but the reciprocal experiment (the viability of a mouse expressing exclusively K-Ras4A from the *KRAS* locus) has not been reported.

Most evidence for an independent function of K-Ras4A has been deduced from the exon 4A KO mouse. Cells isolated from this mouse exhibited impaired apoptosis in vitro in response to etoposide, like the gastrointestinal tract of these mice when treated with etoposide by i.p. injection (25). Similarly, when colonic adenomas were induced in these mice by treatment with 1,2-dimethylhydrazine, mice lacking K-Ras4A had an increase in number and size of colonic adenomas that revealed increased markers of proliferation and decreased markers of apoptosis

(26), suggesting that, despite the highly counterintuitive nature of these findings, WT K-Ras4A can behave like a tumor suppressor. However, a similar study using a mouse genetic model to induce colon carcinomas showed no such effect of K-Ras4A deficiency (27). Another study using a different mouse transgenic at the *KRAS* locus revealed a role for K-Ras4A in tumorigenesis: when the cDNA sequence of K-Ras4B was knocked into the *KRAS* locus, such that only K-Ras4B could be expressed (designated *KRAS^KI*), homozygous *KRAS^KI* mice were resistant to urethane-induced lung carcinogenesis (14). However, the same study called into question the protumor effects of WT K-Ras4A by showing that, when the *KRAS^KI* allele was heterozygous with the *KRAS^LA2* allele that spontaneously recombines to generate oncogenic K-Ras, more lung tumors developed in *KRAS^KI/LA2* than *KRAS^wt/LA2* mice, consistent with a tumor suppressor effect of WT K-Ras4A (14). Thus, the literature on K-Ras4A–deficient mice provides little clarity and no mechanistic understanding of any biological differences that may distinguish the two highly conserved splice variants of the *KRAS* locus.

Because the alternative fourth exons encode the membrane-targeting HVRs of the *KRAS* gene products, we studied the differential subcellular trafficking of the two proteins. We and others have established that the membrane trafficking of N-Ras and H-Ras, which are palmitoylated, differs substantially from that of K-Ras4B, in that N-Ras and H-Ras access the PM through the cytoplasmic surface of the Golgi apparatus, whereas K-Ras4B does not associate with the Golgi (5). The protein palmitoylacyltransferase that modifies N-Ras and H-Ras, DHHC9/GCP16, resides on the Golgi (28), and these Ras isoforms engage in a cycle of palmitoylation/depalmitoylation that takes them to and from the PM (29–31). At steady state, GFP-N-Ras and GFP-H-Ras can clearly be observed on the Golgi in a variety of cultured cells (5).

In contrast, we observed no GFP-K-Ras4A on the Golgi arguing for alternative trafficking.

Laude and Prior (8) observed that the HVRs of each of four Ras isoforms begin with a short PBR and that K-Ras4A has a second short PBR immediately after palmitoylated cysteine 180. We designated these PBRs PB1 and PB2, respectively. We found that substitution of the basic residues in PB1+2 with glutamine generated a K-Ras4A mutant that localized on the PM and Golgi in a manner indistinguishable from that of N-Ras. Conversely, although elimination of the palmitoylation site resulted in mislocalization of GFP-K-Ras4A to internal membranes, this mutant was capable of trafficking to the PM, unlike palmitoylation-deficient N-Ras. Thus, K-Ras4A is unique among Ras isoforms in possessing a hybrid membrane-targeting sequence that contains both functional PBRs and a site of palmitoylation. Importantly, either motif acting alone is sufficient to deliver K-Ras4A to the PM. Palmitoylation of K-Ras4A without any evidence of accumulation on the Golgi suggests that a PM resident palmitoylacyltransferase may modify this protein rather than DHHC9/GCP16. Another striking and unexpected finding was that, whereas PDE6δ could extract K-Ras4B from membranes, it did not affect the localization of K-Ras4A, highlighting the significant differences in their subcellular trafficking. The results reported here require that the comprehensive scheme of the subcellular trafficking of Ras proteins (32) be amended to include a third hybrid pathway used by K-Ras4A (Fig. S9).

Among the most attractive approaches to anti-Ras therapy are those that interfere with membrane targeting. Our data suggest that K-Ras4A plays a significant role in K-Ras–driven tumors and that the mechanism through which K-Ras4A gains access to the PM is distinct from that of K-Ras4B. Accordingly, the search for therapies designed to interfere with oncogenic K-Ras by limiting its access to the PM will have to take into account the two distinct mechanisms of K-Ras trafficking.

Materials and Methods

qPCR. Cultured human cancer cell lines or fresh frozen colon tumor samples (acquired through the Massachusetts General Hospital Tissue Repository) were collected, and RNA was isolated using the RNeasy Plus Mini Kit (QIAGEN). Reverse transcription was performed on 2–5 mg total RNA using the SuperScript III First-Strand Synthesis System (Invitrogen); 2% of the reverse transcription product was used for real-time PCR using Maxima SYBR Green qPCR Master Mix (Thermo Scientific) and an MyiQ Thermal Cycler (Bio-Rad) with primers designed to produce amplicons within K-Ras4A and K-Ras4B. Results were normalized to a standard curve generated from a dilution series of GFP-K-Ras4A and GFP-K-Ras4B plasmid DNA included in each set of real-time PCR reaction as well as 18S or β-actin cDNA.

Primer sequences are as follows: for total K-Ras (X3), forward: 5′-tacagtgcaatgagggacca-3′, reverse: 5′-tcctgagcctgttttgtgtct-3′; for K-Ras4A (X4A; 4A), forward: 5′-agacacaaaacaggctcagga-3′, reverse: 5′-ttcacacagccaggagtcttt-3′; for K-Ras4B (X4B), forward: 5′-agacacaaaacaggctcagga-3′, reverse: 5′-tcttcttttaccatctttgctca-3′; for K-Ras4B (4B), forward: 5′-gactgggagggctttcttt-3′, reverse: 5′-gcatcatcaaccaccctgtct-3′; for 18S RNA, forward: 5′-ggacacggacaggattgaca-3′, reverse: 5′-acccacggaatcgagaaaga-3′; for β-actin, forward: 5′-ggggtgttgaaggtctcaaa-3′, reverse: 5′-ggcatcctcaccctgaagta-3′.

Antibody Development. Custom rabbit polyclonal antibodies were developed by Bio-Synthesis, Inc., including custom peptide synthesis and conjugation. Peptide sequences of epitopes are as follows: for K-Ras4A, 161-REIRQYRLKKISKEEKTPGC-180; for K-Ras4B, 166-HKEKMSKDGKKKKKKSKTKC-186.

Confocal Microscopy. Live cells were seeded in 35-mm dishes containing no. 0 glass coverslips over 15-mm cutouts (MatTek) and transfected with the relevant constructs. For pharmacological treatment, 2-bromopalmitate was used at 50 μM for 3 h. Cells were imaged with a Zeiss 510 laser-scanning confocal microscope (Carl Zeiss MicroImaging, Inc.) using a 63×, N.A. 1.4 objective and a humidified metabolic chamber maintained at 37 °C and 5% CO₂ (Pecon GmbH). Images were processed with Adobe Photoshop CS6.

Additional methods can be found in SI Materials and Methods.

1. Prior IA, Lewis PD, Mattos C (2012) A comprehensive survey of Ras mutations in cancer. *Cancer Res* 72(10):2457–2467.
2. Vigil D, Cherfils J, Rossman KL, Der CJ (2010) Ras superfamily GEFs and GAPs: Validated and tractable targets for cancer therapy? *Nat Rev Cancer* 10(12):842–857.
3. Willumsen BM, Christensen A, Hubbert NL, Papageorge AG, Lowy DR (1984) The p21 ras C-terminus is required for transformation and membrane association. *Nature* 310(5978):583–586.
4. Wright LP, Philips MR (2006) Thematic review series: Lipid posttranslational modifications. CAAX modification and membrane targeting of Ras. *J Lipid Res* 47(5):883–891.
5. Choy E, et al. (1999) Endomembrane trafficking of ras: The CAAX motif targets proteins to the ER and Golgi. *Cell* 98(1):69–80.
6. Hancock JF, Paterson H, Marshall CJ (1990) A polybasic domain or palmitoylation is required in addition to the CAAX motif to localize p21ras to the plasma membrane. *Cell* 63(1):133–139.
7. Bivona TG, et al. (2006) PKC regulates a farnesyl-electrostatic switch on K-Ras that promotes its association with Bcl-XL on mitochondria and induces apoptosis. *Mol Cell* 21(4):481–493.
8. Laude AJ, Prior IA (2008) Palmitoylation and localisation of RAS isoforms are modulated by the hypervariable linker domain. *J Cell Sci* 121(Pt 4):421–427.
9. Pells S, et al. (1997) Developmentally-regulated expression of murine K-ras isoforms. *Oncogene* 15(15):1781–1786.
10. Plowman SJ, et al. (2006) K-ras 4A and 4B are co-expressed widely in human tissues, and their ratio is altered in sporadic colorectal cancer. *J Exp Clin Cancer Res* 25(2):259–267.
11. Plowman SJ, et al. (2003) While K-ras is essential for mouse development, expression of the K-ras 4A splice variant is dispensable. *Mol Cell Biol* 23(24):9245–9250.
12. Shimizu K, et al. (1983) Structure of the Ki-ras gene of the human lung carcinoma cell line Calu-1. *Nature* 304(5926):497–500.
13. Voice JK, Klemke RL, Le A, Jackson JH (1999) Four human ras homologs differ in their abilities to activate Raf-1, induce transformation, and stimulate cell motility. *J Biol Chem* 274(24):17164–17170.
14. To MD, et al. (2008) Kras regulatory elements and exon 4A determine mutation specificity in lung cancer. *Nat Genet* 40(10):1240–1244.
15. Capon DJ, et al. (1983) Activation of Ki-ras2 gene in human colon and lung carcinomas by two different point mutations. *Nature* 304(5926):507–513.
16. Butz JA, Roberts KG, Edwards JS (2004) Detecting changes in the relative expression of KRAS2 splice variants using polymerase colonies. *Biotechnol Prog* 20(6):1836–1839.
17. Shirasawa S, Furuse M, Yokoyama N, Sasazuki T (1993) Altered growth of human colon cancer cell lines disrupted at activated Ki-ras. *Science* 260(5104):85–88.
18. Mor A, Philips MR (2006) Compartmentalized Ras/MAPK signaling. *Annu Rev Immunol* 24:771–800.
19. Chandra A, et al. (2012) The GDI-like solubilizing factor PDE6δ sustains the spatial organization and signalling of Ras family proteins. *Nat Cell Biol* 14(2):148–158.
20. Schmick M, et al. (2014) KRas localizes to the plasma membrane by spatial cycles of solubilization, trapping and vesicular transport. *Cell* 157(2):459–471.
21. Esteban LM, et al. (2001) Targeted genomic disruption of H-ras and N-ras, individually or in combination, reveals the dispensability of both loci for mouse growth and development. *Mol Cell Biol* 21(5):1444–1452.
22. Johnson L, et al. (1997) K-ras is an essential gene in the mouse with partial functional overlap with N-ras. *Genes Dev* 11(19):2468–2481.
23. Koera K, et al. (1997) K-ras is essential for the development of the mouse embryo. *Oncogene* 15(10):1151–1159.
24. Potenza N, et al. (2005) Replacement of K-Ras with H-Ras supports normal embryonic development despite inducing cardiovascular pathology in adult mice. *EMBO Rep* 6(5):432–437.
25. Plowman SJ, et al. (2006) The K-Ras 4A isoform promotes apoptosis but does not affect either lifespan or spontaneous tumor incidence in aging mice. *Exp Cell Res* 312(1):16–26.
26. Luo F, et al. (2010) K-ras exon 4A has a tumour suppressor effect on carcinogen-induced murine colonic adenoma formation. *J Pathol* 220(5):542–550.
27. Patek CE, et al. (2008) Mutationally activated K-ras 4A and 4B both mediate lung carcinogenesis. *Exp Cell Res* 314(5):1105–1114.
28. Swarthout JT, et al. (2005) DHHC9 and GCP16 constitute a human protein fatty acyltransferase with specificity for H- and N-Ras. *J Biol Chem* 280(35):31141–31148.
29. Goodwin JS, et al. (2005) Depalmitoylated Ras traffics to and from the Golgi complex via a nonvesicular pathway. *J Cell Biol* 170(2):261–272.
30. Rocks O, et al. (2010) The palmitoylation machinery is a spatially organizing system for peripheral membrane proteins. *Cell* 141(3):458–471.
31. Rocks O, et al. (2005) An acylation cycle regulates localization and activity of palmitoylated Ras isoforms. *Science* 307(5716):1746–1752.
32. Ahearn IM, Haigis K, Bar-Sagi D, Philips MR (2012) Regulating the regulator: Post-translational modification of RAS. *Nat Rev Mol Cell Biol* 13(1):39–51.